Food and Chemical Toxicology 124 (2019) 101–111

Contents lists available at ScienceDirect

Food and Chemical Toxicology

journal homepage: www.elsevier.com/locate/foodchemtox

Resveratrol analog, *N*-(4-methoxyphenyl)-3,5-dimethoxybenzamide induces G_2/M phase cell cycle arrest and apoptosis in HeLa human cervical cancer cells

Kyung-Won Lee[a,b,1], Kyung-Sook Chung[a,1], Jeong-Hun Lee[a,b], Jung-Hye Choi[b,c], Sang Yoon Choi[d], Sanghee Kim[e], Jae Yeol Lee[f], Kyung-Tae Lee[a,b,*]

[a] Department of Pharmaceutical Biochemistry, College of Pharmacy, Kyung Hee University, 26 Kyungheedae-ro, Seoul, 02447, Republic of Korea
[b] Department of Life and Nanopharmaceutical Science, College of Pharmacy, Kyung Hee University, 26 Kyungheedae-ro, Seoul, 02447, Republic of Korea
[c] Oriental Pharmaceutical Science, College of Pharmacy, Kyung Hee University, 26 Kyungheedae-ro, Seoul, 02447, Republic of Korea
[d] Korea Food Research Institute, 245 Nongsaengmyeong-ro, Wanju, 55365, Republic of Korea
[e] College of Pharmacy, Seoul National University, 1 Gwanak-ro, Seoul, 08826, Republic of Korea
[f] Research Institute for Basic Sciences and Department of Chemistry, College of Sciences, Kyung Hee University, 26 Kyungheedae-ro, Seoul, 02447, Republic of Korea

ARTICLE INFO

Keywords:
N-(4-Methoxyphenyl)-3,5-dimethoxybenamide
Resveratrol
Antiproliferation
G2/M arrest
Apoptosis

ABSTRACT

In this study, several resveratrol analogs were synthesized and evaluated in search of a more effective anti-proliferative resveratrol analog. Among the evaluated resveratrol analogs, we have identified N-(4-methoxyphenyl)-3,5-dimethoxybenamide (MPDB) as a potent anti-proliferative compound. Treatment with MPDB resulted in G_2/M phase cell cycle arrest, which was accompanied by alteration of G_2/M-related protein expression and phosphorylation. MPDB-induced G_2/M arrest was blocked by transfection of ATM/ATR siRNAs, indicating the critical role of ATM/ATR in G_2/M phase arrest. In addition, treatment with MPDB displayed the activation of caspase and decreased Bcl-xl protein expression after 20 h in HeLa cells. Moreover, MPDB increased cytosolic cytochrome *c* release and Fas and Fas-L protein expression, indicating intrinsic and extrinsic apoptosis pathway, respectively. These results suggest that MPDB is a new and potent compound that induces ATM/ATR-dependent G_2/M phase cell cycle arrest and apoptosis, implicating it as a putative candidate in the investment of cervical cancer therapy.

1. Introduction

The adult human body consists of about 50–100 trillion cells. Each day, several billions of these cells divide in two to replace the billions of cells that die, and are removed. The correlation between the cell cycle and cancer is obvious: cell cycle machinery controls cell proliferation, and cancer is a disease of inappropriate cell proliferation (Asghar et al., 2015). Basically, all cancers permit the existence of too many cells, but this cell number excess is linked in a vicious cycle with a reduction in sensitivity to signals that normally tell a cell to adhere, differentiate, or die. This combination of altered properties increases the difficulty of deciphering which changes are primarily responsible for causing cancer. There are an estimated 520,000 new cervical cancer cases per year worldwide (Torre et al., 2015). Although it is hoped that in the future, human papillomavirus vaccines and cancer drug will prevent cervical cancer, the treatment options for patients with metastatic, persistent, or recurrent disease are very limited, and cervical cancer is currently the third leading cause of death among women in developed countries. In the advanced stage, cervical cancer is a chemotherapy-refractory disease for which durable palliation or cure is rarely achieved (Ramondetta, 2013). In this regard, there is urgent need to develop a new strategy for the disease.

Cells progress the cell cycle in several well-controlled phases (Diaz-Moralli et al., 2013). In the G_1 phase, cells commit to enter the cell cycle, and prepare to duplicate their DNA in S phase. After S phase, cells enter the G_2 phase, where repair might occur, along with preparation for mitosis in M phase. In the M phase, chromatids and daughter cells separate. After M phase, the cells can enter G_1 or G_0, a quiescent phase. Cell cycle progression and cell division is under the control of a tightly regulated network of cell division kinases and numerous surveillance

* Corresponding author. Department of Pharmaceutical Biochemistry, College of Pharmacy, Kyung Hee University, 26 Kyungheedae-ro, Seoul, 02447, Republic of Korea.
E-mail address: ktlee@khu.ac.kr (K.-T. Lee).
[1] Lee and Chung contributed to the work equally and should be regarded as co-first authors.

https://doi.org/10.1016/j.fct.2018.11.062
Received 2 July 2018; Received in revised form 27 November 2018; Accepted 29 November 2018
Available online 30 November 2018
0278-6915/

mechanisms, the so-called checkpoints. Cyclin-dependent kinases (CDKs) and regulatory subunits cyclins control the cell cycle progression, which is triggered by phosphorylation of Rb. Members of the Cip/Kip family of CDK inhibitor (CDKI), such as $p21^{Cip1/Waf1}$ and $p27^{Kip1}$, disrupt these interactions, and inhibit cell cycle progression. The regulation of the cell cycle is tightly linked to the control of cell death. Cyclins and CDKs can modulate apoptotic cell death pathways, and CDK inhibitors also play the role of a key regulator in carcinogenesis and the promotion of tumors (Hydbring et al., 2016). This multiplicity of regulatory mechanisms allows cell cycle progression to be responsive to a diverse array of external and internal factors, and induces prevention of cell cycle progression, leading to apoptosis when DNA damage would make such progression harmful to the cell. Resveratrol (3,5,4′-trihydroxy-trans-stilbene) is a polyphenolic phytoalexin, a class of antibiotic compounds that are produced as a part of the plant's defense system against disease, and found in grapes and berries of the *Vaccinum* species (Rossi et al., 2018). Resveratrol has been extensively considered for its various biological activities, like cardiovascular protection, anti-oxidative, anti-inflammatory, and anti-aging activities (Carter et al., 2014). In addition, resveratrol has also been observed to possess a chemopreventive activity against all the three major stages of carcinogenesis of initiation, promotion, and progression, and inhibits growth and induces apoptosis, as well as cell cycle arrest, in various human cancer cell lines (Estrov et al., 2003; Trincheri et al., 2007). Moreover, several studies have observed that resveratrol and its analogs induced DNA damage in various human cancer cell lines, and that it could bind to DNA, and cleave or damage DNA in a Cu^{2+} dependent pathway (Azmi et al., 2005; Zheng et al., 2006). We also previously reported that resveratrol analog (*E*)-8-acetoxy-2-[2-(3,4-diacetoxyphenyl)ethenyl]-quinazoline induced cell cycle arrest through the activation of ATM/ATR in human cervical carcinoma HeLa cells and apoptosis via Fas-mediated pathway in HL-60 human leukemia cells (Kim et al., 2015; Park et al., 2016). In this study, we screened the cytotoxic activity of various resveratrol analogs, and elucidated the mechanism involving the induction of cell cycle arrest and apoptosis on HeLa human cervical cancer cells.

2. Materials and methods

2.1. Materials

RPMI 1640 medium, FBS, penicillin, and streptomycin were obtained from Life Technologies (Grand Island, NY, USA) and broad caspase inhibitor z-VAD-fmk was from Calbiochem (Bad Soden, Germany). Antibodies for CDK2, Cyclin B1, wee1, p53, $p21^{Cip1/Waf1}$, p27, caspase-3, PARP, Bcl-2, Bcl-xL, Fas, Fas-L, FLIP, and β-actin were purchased from Santa Cruz Biotechnology (Santa Cruz, CA, USA). Antibodies for p-CDK1 (Tyr15), CDK1, p-Cdc25C (Ser216), Cdc25C, p-Chk1 (Ser345), p-Chk2 (Thr68), Chk1, Chk2, p-p53 (Ser15), p-p53 (Ser20), p-H_2AX (Ser139), p-ATM (Ser1981), p-ATR (Ser428), ATM, ATR and caspase-9 were purchased from Cell Signaling Technology (Beverly, MA, USA) In addition, antibodies for caspase-9 and cytochrome *c* were purchased from BD Biosciences, Pharmingen (San Diego, CA, USA). Resveratrol, lactacystin, propidium iodide (PI), 3-(4,5-Dimethylthiazol-2-yl)-2,5-diphenyltetrazolium bromide (MTT), and other reagents were purchased from Sigma (St. Louis, MO, USA). The resveratrol analogs were synthesized using the previously reported method (Table 1, (Choi et al., 2006; Choi et al., 2004).

Compound **1**. *2,6-dimethoxy-N-phenylbenzamide*: mp 169.65–171 °C; ^{1}H-NMR ($CDCl_3$): δ 7.58 (d, 2H, *J* = 7.5 Hz), 7.36 (br s, 1H), 7.26 (dd, 3H, *J* = 16.5, 8.4 Hz), 7.05 (t, 1H, *J* = 7.4 Hz), 6.53 (d, 2H, *J* = 8.4 Hz), 3.77 (s, 6H).

Compound **2**. *N-(4-methoxyphenyl)-3,5-dimethoxybenzamide (MPDB)*: mp 94.6–95.75 °C; ^{1}H NMR ($CDCl_3$): δ 8.11 (s, 1H), 7.51 (d, 2H, *J* = 8.7 Hz), 6.94 (d, 2H, *J* = 2.4 Hz), 6.84 (m, 2H), 6.55 (t, 1H, *J* = 2.4 Hz), 3.78 (s, 3H), 3.76 (s, 6H).

Compound **3**. *2,6-Dimethoxy-N-(4-methoxyphenyl)benzamide*: mp 151.37–157.87 °C; ^{1}H NMR ($CDCl_3$): δ 7.52–7.47 (m, 2H), 7.28 (s, 1H), 7.24 (t, 1H, *J* = 8.4 Hz), 6.81 (m, 2H), 6.52 (d, 2H, *J* = 8.4 Hz), 3.76 (s, 6H), 3.73 (s, 3H).

Compound **4**. *2,6-Dimethoxy-N-(4-butoxyphenyl)benzamide*: mp 124.8–126.25 °C; ^{1}H NMR (CDCl3): δ 7.55 (m, 2H), 7.34–7.28 (m, 2H), 6.88 (m, 2H), 6.61 (s, 1H), 6.58 (s, 1H), 3.96 (t, 2H, *J* = 6.6 Hz), 3.84 (s, 6H), 1.75 (m, 2H), 1.50 (m, 2H), 0.98 (t, 3H, *J* = 7.2 Hz).

Compound **5**. *N-(3,4-Dimethoxyphenyl)-2,4,6-trimethoxybenzamide*: mp 176.05–177.35 °C; ^{1}H NMR ($CDCl_3$): δ 7.64 (d, 1H, *J* = 2.4 Hz), 7.41 (s, 1H), 6.91–6.80 (m, 2H), 6.15 (s, 2H), 3.92 (s, 3H), 3.87 (s, 3H), 3.85 (s, 3H), 3.83 (s, 3H).

Compound **6**. *2,5-Dimethoxyl-N-(4-methoxyphenyl)benzamide*: mp 94.2–95.35 °C; ^{1}H NMR ($CDCl_3$): δ 7.85 (d, 1H, *J* = 2.7 Hz), 7.61–7.56 (m, 3H), 7.03 (dd, 1H, *J* = 2.7 Hz; 2.7 Hz), 6.97 (d, 1H, *J* = 9.0 Hz), 6.91 (d, 2H, *J* = 9.0 Hz), 4.01 (s, 3H), 3.85 (s, 3H), 3.82 (s, 3H).

Compound **7**. *2,4-Dimethoxy-N-(4-methoxyphenyl)benzamide*: mp 98.25–99.5 °C; ^{1}H NMR ($CDCl_3$): δ 9.56 (s, 1H), 8.26 (d, 1H, *J* = 8.7 Hz), 7.57 (m, 2H), 6.89 (m, 2H), 6.65 (dd, 1H, *J* = 2.4 Hz; 2.4 Hz), 6.53 (d, 1H, *J* = 2.4 Hz), 4.02 (s, 3H), 3.87 (s, 3H), 3.81 (s, 3H).

Compound **8**. *2-(2-Methoxybenzoylamino)benzoic acid methyl ester*: mp 67.95–69.3 °C; ^{1}H NMR ($CDCl_3$): δ 12.18 (s, 1H), 8.94 (dd, 1H, *J* = 0.9 Hz; 1.2 Hz), 8.20 (dd, 1H, *J* = 1.8 Hz; 1.8 Hz), 8.03 (dd, 1H, *J* = 1.8 Hz; 1.8 Hz), 7.57 (m, 1H), 7.47 (m, 1H), 7.09 (m, 2H), 7.02 (m, 1H), 4.07 (s, 3H), 3.91 (s, 3H).

2.2. Cell culture and MTT assay

HeLa, CaSki and SiHa human cervical carcinoma, HL-60 human leukemia, and MRC5 human normal lung fibroblast cell lines were obtained from the Korean Cell Line Bank (KCLB, Seoul, Korea) and immortalized ovarian surface epithelial (IOSE-80PC) normal cell were kindly provided by Dr. Auer-sperg (University of British Columbia, Canada) and A. Godwin (Fox Chase Cancer Center, Philadelp hia, PA, USA). Cells were cultured in RPMI 1640 medium (Life technologies Inc. Grand Island, NY, USA) with 10% heat-inactivated fetal bovine serum (FBS), penicillin (100 units/ml) and streptomycin sulfate (100 μg/ml) (Life Technologies Inc.) in a 37 °C, CO_2 incubator in the presence or absence of the chemicals. The cytotoxicity was measured using a MTT assay as previously described (Chung et al., 2010). Briefly, the 5,000 cells were seeded in each well containing 100 μl of the RPMI medium supplemented in a 96-well plate. After 24 h, various concentrations of MPDB were added. After 48 h, 50 μl of MTT (5 mg/ml stock solution) was added and the plates were incubated for an additional 4 h. The medium was discarded and the formazan blue, which was formed in the cells, was dissolved with 100 μl DMSO. The optical density was measured by spectrometer reader at 540 nm.

2.3. Colony formation assay

Colony formation assay was performed as previously described (Jang et al., 2017). HeLa cells were seed in 60 mm dishes (1000 cells per dish). The next day, cells were treated with various concentration of MPDB. After treatment of MPDB for 24 h in HeLa cells, medium was changed. The cells kept growing in fresh medium without any treatment during 10 days. The medium was discarded and the colonies, which was formed in the plate were fixed with 100% methanol for 10 min and stained with 0.1% crystal violet solution for 1 h. After washing with PBS, the dishes were air-dried and the colonies were counted.

2.4. Analysis of cell cycle progression

HeLa cells were seed in 60 mm dishes (300,000 cells per dish). The next day, cells were treated with 35μ MPDB for 25 h. After treatment

Table 1
In vitro cytotoxic activity of resveratrol and its amide analogs on the proliferation of various cancer cells.

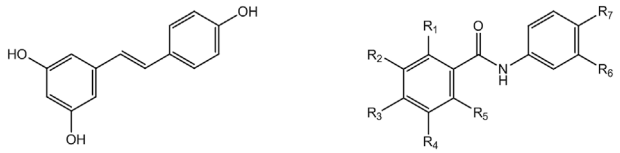

Resveratrol **Amide analogs**

Compound	Substituent							IC_{50} (μM)	
	R1	R2	R3	R4	R5	R6	R7	HeLa	HL-60
1	OCH_3	H	H	H	OCH_3	H	H	> 300	> 300
2	H	OCH_3	H	OCH_3	H	H	OCH_3	38.9	47.7
3	OCH_3	H	H	H	OCH_3	H	OCH_3	> 300	> 300
4	OCH_3	H	H	H	OCH_3	H	OC_3H_7	> 300	> 300
5	OCH_3	H	OCH_3	H	OCH_3	OCH_3	OCH_3	> 300	101.8
6	OCH_3	H	H	OCH_3	H	H	OCH_3	> 300	101.6
7	OCH_3	H	OCH_3	H	H	H	OCH_3	> 300	110.5
8	H	H	CH_3	H	H	H	$COOCH_3$	> 300	> 300
Resveratrol								152.4	64.1

with or without MPDB, cells were harvested and fixed in 70% ethanol for 1 h on ice. After washing with PBS, cells were labeled with PI (50 μg/ml) in the presence of RNase A (100 μg/ml) and incubated at room temperature in the dark for 30 min and analyzed using the fluorescence-activated cell sorting (FACS) cater-plus Flow cytometry (Becton Dickinson Co., Germany).

2.5. Terminal deoxynucleotidyl transferase–mediated dUTP nick end labeling (TUNEL) assay

HeLa cells were seed in 4 well chamber slide (5000 cells per well). The next day, cells were treated with various concentration of MPDB for 48 h, and TUNEL assay was carried out according to the manufacturer's instructions (in situ cell death detection kit, POD, Roche, Germany). Briefly, after fixation with 25% formaldehyde, permeabilization buffer was treated and then immersed in TUNEL reaction mixture for 1 h at 37 °C under humidified atmosphere in the dark. The slides were then washed with PBS and stained cells indicating apoptotic death cells were determined using an Olympus microscope (OLYMPUS cellSens Standard 1.9., Tokyo, Japan) with Bio-rad Quantity One® Software (ver 4.6.3) and cell viability was examined from cell death ratio.

2.6. Small interfering RNA transfection

RNA interference of control, ATM, ATR and p53 was performed using 21 bp (including a 2-deoxynucleotide overhang) siRNA duplexes purchased from Invitrogen. HeLa cells were transfected with 100 nM siRNA duplexes using Lipofectamine™ RNAiMAX (Invitrogen, Carlsbad, CA, USA) according to the manufacturer's recommendations. After 48 h of transfection, cells were treated with or without MPDB for 15 h.

2.7. Western blot analysis

Cells were lysed in ice-cold cell lysis buffer (50 mM HEPES pH 7.0, 250 mM NaCl, 5 mM EDTA, 0.1% triton X-100, 0.5 mM DTT, 5 mM NaF, 0.5 mM sodium orthovanadate, 0.1 mM PMSF, 20 μg/ml aprotinin, and 20 μg/ml leupeptin) for 20 min on ice. Cell debris was removed by microcentrifugation (10,000 *g*, 5 min), followed by quick freezing of the supernatants. Protein concentration was determined by Bio-Rad protein assay reagent. Cellular proteins (20–40 μg) were electroblotted onto nitrocellulose membrane following separation on a 10–12% SDS-polyacrylamide gel electrophoresis. The immunoblot was incubated overnight with blocking solution (5% skim milk in Tris-buffered saline containing Tween20 (TTBS)) then incubated for further 4 h with a 1:1000 dilution of primary an tibodies. Blots were washed three times with TTBS, then incubated with a 1:1000 dilution of horseradish peroxidase-conjugated secondary antibody for 1 h at room temperature. Blots were washed again three times with TTBS, and developed by enhanced chemiluminescence (GE Healthcare, Milwaukee, WI, USA).

2.8. DAPI assay

DAPI assay were modified and performed as described previous report (Cho et al., 2009). Cells were lysed in a solution of 1 M Tris-HCl (pH 7.4) and 0.5 M EDTA that contained 0.5% (w/v) Triton X-100 for 20 min on ice. The lysate and the supernatant after centrifugation at 25,000 *g* for 20 min were sonicated for 20 s. The level of DNA in each fraction was measured by a fluorometric method with the fluorescent reagent 0.1 μg/ml DAPI. The amount of the fragmented DNA was calculated as the ratio of the amount of DNA in the supernatant to that in the lysate.

2.9. Preparation of cytosolic and mitochondrial fractions

Cells were lysed with 100 μl of mitobuffer (20 mM HEPES, 1 mM EGTA, 1 mM EDTA, 10 mM KCl, 1.5 mM $MgCl_2$, 1 mM DTT, 0.1 mM PMSF, 2 μg/ml leupeptin, 2 μg/ml pepstain, 2 μg/ml aprotinin) and homogenized with the pestle on ice. The homogenate was centrifuged at 845 *g* for 20 min at 4 °C and the supernatant was centrifuged at 11,363 *g* for 20 min at 4 °C. The resulting pellet was lysed with mitobuffer and represented the mitochondrial fraction (M). The supernatant was centrifuged further at 18,407 *g* for 20 min at 4 °C. The final supernatant represented the cytosolic fraction (C).

2.10. Statistical analysis

Data presented are the means ± S.D. of results from three independent experiments with similar patterns. $^{*}P < 0.05$, $^{**}P < 0.01$ and $^{***}P < 0.001$ *vs* control group, $^{\#}P < 0.05$, $^{\#\#}P < 0.01$ and $^{\#\#\#}P < 0.001$ *vs* MPDB-treated group; significance of difference between treated groups by Student's *t*-test.

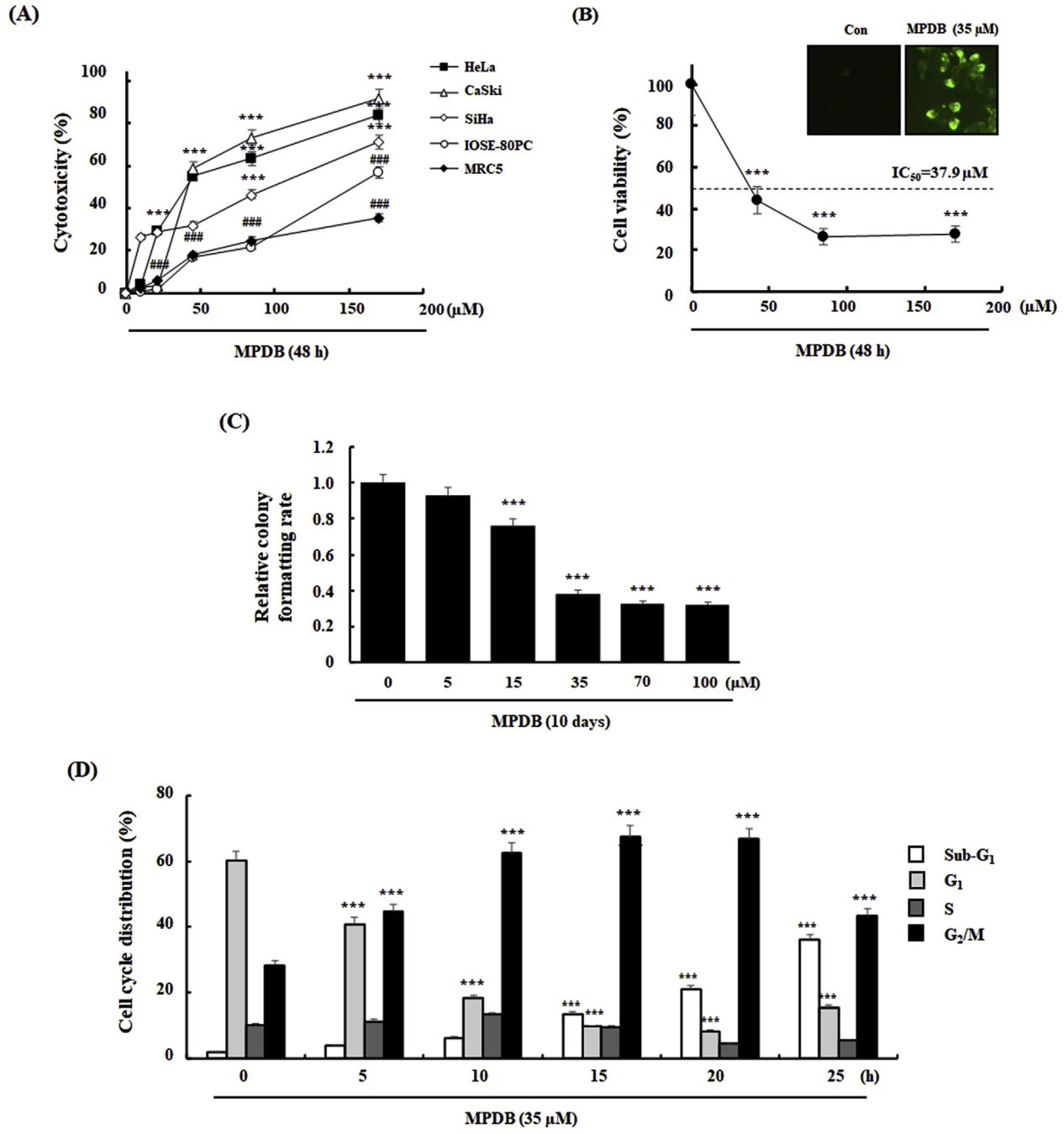

Fig. 1. Effect of MPDB on the growth inhibition and cell cycle distribution at G_2/M in HeLa cells. (A) Human cervical carcinoma HeLa, CaSki and SiHa, human normal lung fibroblast MRC5, and IOSE-80PC normal cells were treated with various concentration of MPDB for 48 h, and cytotoxicity was determined by MTT assay. (B) HeLa cells were treated with various concentration of MPDB for 48 h, and cell viability was examined by TUNEL assay. (C) Colony formation was performed after treatment of MPDB in HeLa cells. (D) Cell cycle distribution was analyzed after treatment of MPDB in HeLa cells. Data are presented as mean ± SD of three independent experiments. $^{***}P < 0.001$ vs. the control group; $^{###}P < 0.001$ vs. the MPDB-treated HeLa cell group.

3. Results and discussion

3.1. MPDB attenuated the growth and cell cycle progression at G_2/M phase in HeLa cells

Resveratrol is a class of polyphenolic compounds with a relatively broad distribution in plants and various human foods, including red wines, peanuts, and blueberries (Shukla and Singh, 2011). It has been shown to have potential activity of cancer prevention, and to induce cell cycle arrest or apoptosis in various cancer cells. With reference to these chemopreventive effects of resveratrol, we have tried to prepare resveratrol analogs with more potent anti-proliferative activity. Here, resveratrol analogs were synthesized using the previously reported method (Choi et al., 2004, 2006), and investigated in search of more efficient and potent chemopreventive agents than resveratrol. To verify the inhibitory effects of resveratrol analogs on cancer cell growth, we determined the cytotoxicity of resveratrol and its analogs using MTT assay. Table 1 shows that the evaluated analogs revealed varying degrees of cytotoxicity, as assessed using their IC_{50} values. Among the compounds, MPDB showed more potent cytotoxicity than resveratrol on HeLa and HL-60 cells. This enhanced activity is understandable in lieu of literature reports showing resveratrol which possess three polar

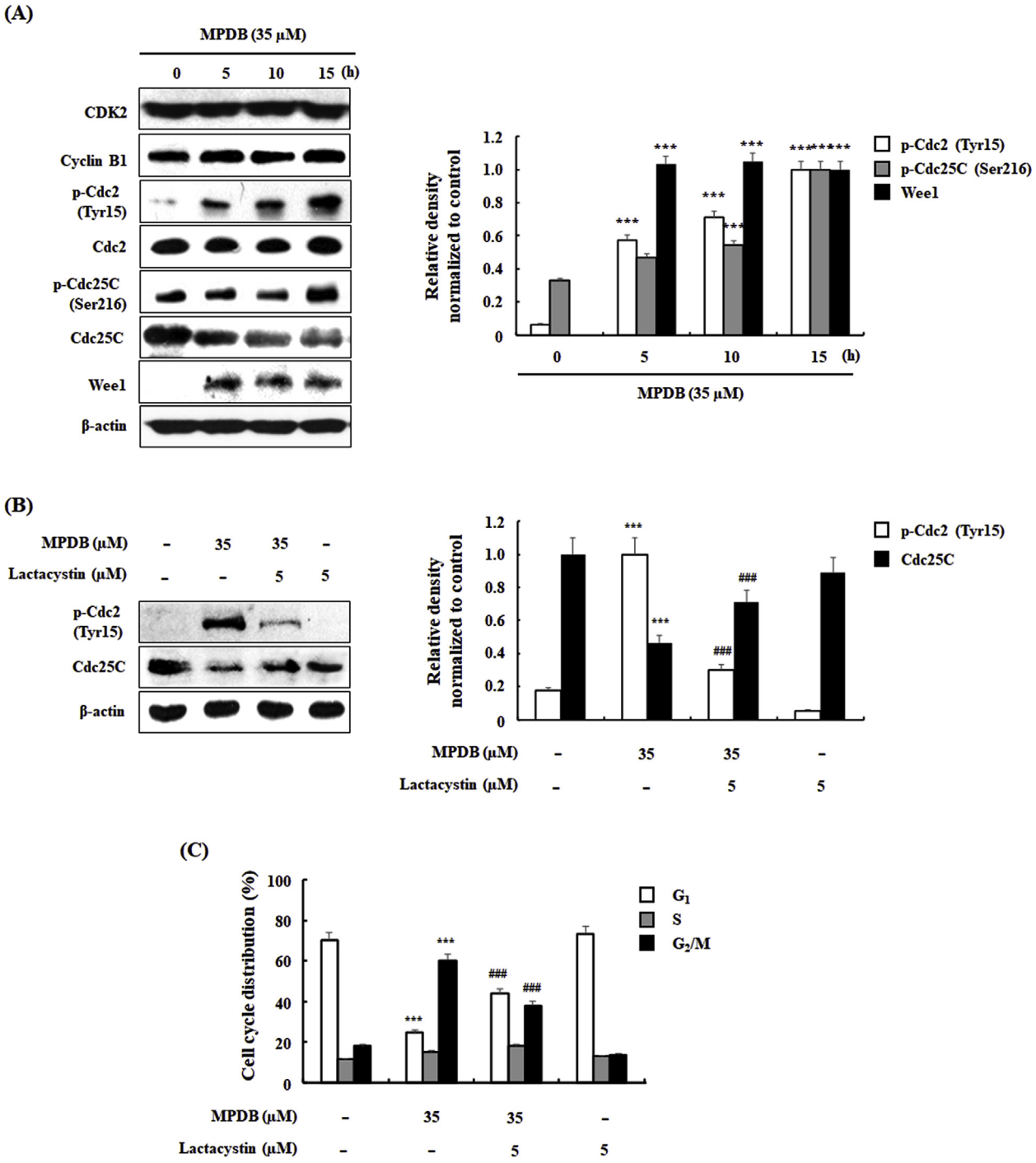

Fig. 2. Effect of MPDB on the G_2/M arrest-related protein expression in HeLa cells. (A) Cells were treated with 35 μM MPDB for the indicated time, and protein expression levels were examined using western blot analysis. β-Actin was used as an internal control. (B) and (C) Cells were pretreated for 2 h with or without 5 μM lactacystin, followed by 35 μM MPDB treatment for 15 h. Protein lysates that were prepared from cells were subjected to western blot analysis, to determine representative proteins. Cell cycle distribution was stained with PI, and analyzed by flow cytometry, as described in the Materials and Methods. Ratio of relative density was determined by densitometric analysis program (Bio-rad Quantity One® Software) normalized to β-actin. Data are presented as mean ± SD of three independent experiments. $^{***}P < 0.001$ vs. the control group, $^{\#\#\#}P < 0.001$ vs. the MPDB-treated group.

hydroxyl groups elicits poor pharmacokinetics and lower cytotoxic activity that the 3,5,4′-trimethoxystilbene in which the three hydroxyl groups were converted to methoxy groups (Hassan et al., 2019). Thus, while the clinical activity of resveratrol is not confirmed, the methylated analogs has shown a proven in vitro and in vivo activity. This might arise from the decreased polarity which enhance compound crossing of cell membrane to reach its molecular target and/or enhanced binding affinity. Methoxy groups possess the ability to form hydrophobic interactions which cannot be established by the hydroxyl groups. Therefore, if binding to the molecular target/receptor is depending on accepting hydrogen bonds as well as the formation of hydrophobic Van der Waals interactions, methoxy derivatives would elicit enhanced interaction with the molecular target/receptor. The desired anti-proliferative agent would induce cytotoxicity in tumor cells with little effect in normal cells, and thus would be devoid of undesirable side effects. To check whether MPDB shows cytotoxicity on normal cells

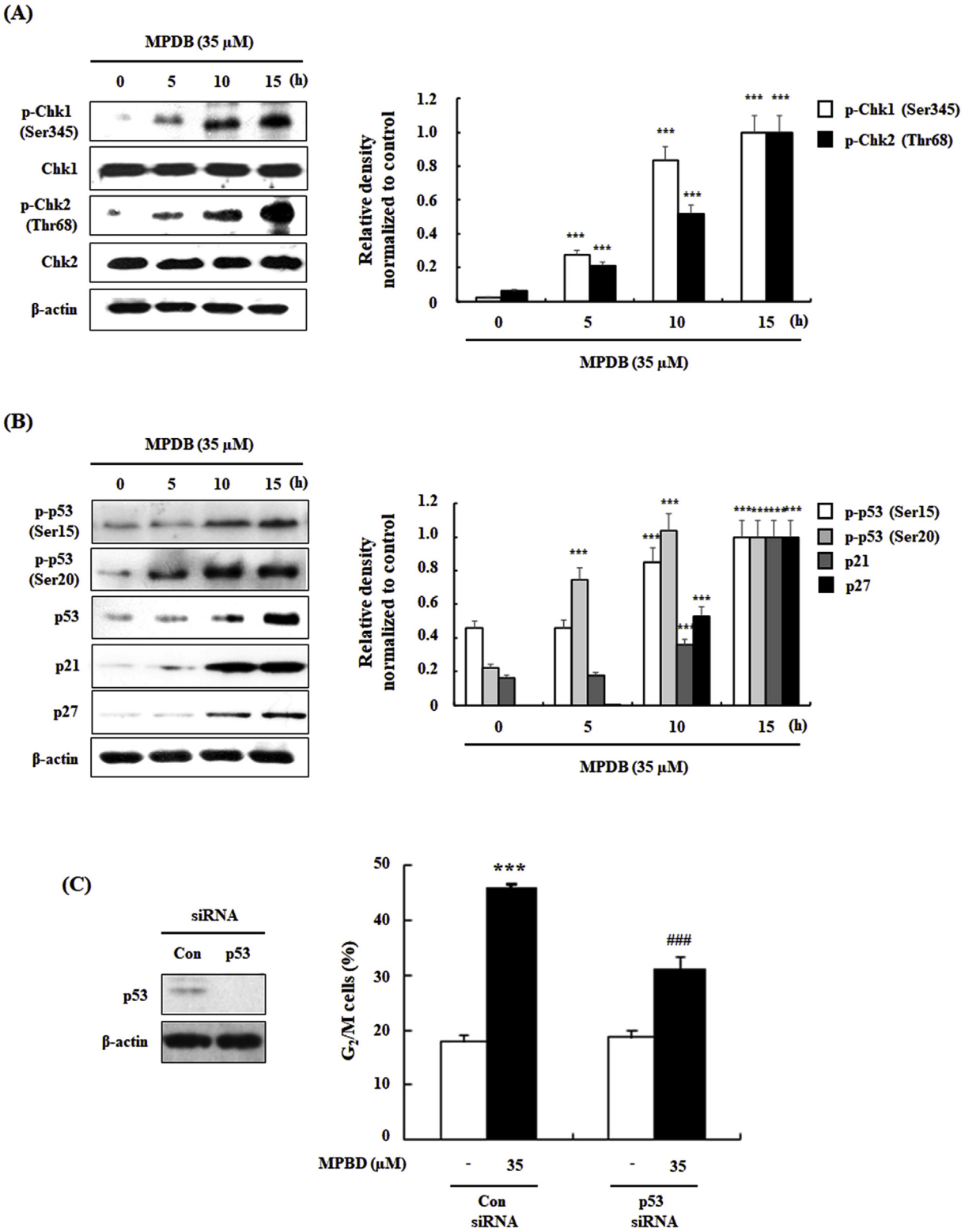

Fig. 3. Effect of MPDB on checkpoint proteins and CDKIs in HeLa cells. (A and B) Cells were treated with 35 μM MPDB for the indicated time. The protein expression levels were examined using western blot analysis. β-Actin was used as an internal control. Ratio of relative density was determined by densitometric analysis program (Bio-rad Quantity One® Software) normalized to β-actin. (C) Control and p53 siRNA-transfected HeLa cells were treated with 35 μM MPDB for 15 h. The expression levels of p53 were determined using western blot analysis. HeLa cells were transfected with control and p53 siRNA for 24 h. Cell cycle distribution was analyzed by flow cytometry, as described in the Materials and Methods. Data are presented as mean ± SD of three independent experiments. $^{***}P < 0.001$ vs. the control group, $^{###}P < 0.001$ vs. the MPDB-treated group.

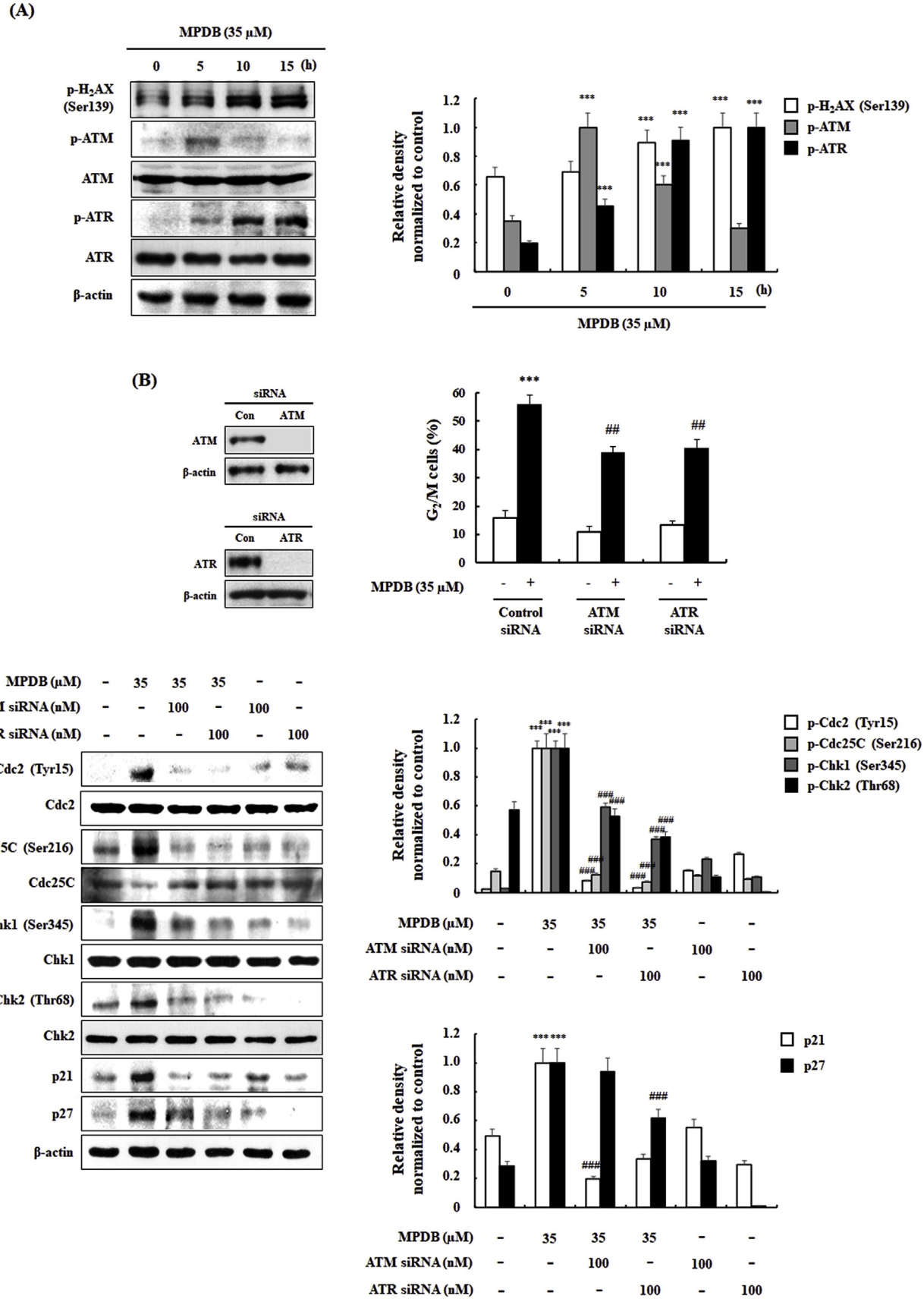

(caption on next page)

Fig. 4. Effect of MPDB on DNA damage and ATM/ATR-dependent G_2/M arrest in HeLa cells. (A) The protein expression levels were examined using western blot analysis. β-Actin was used as an internal control. (B and C) HeLa cells were transfected with control, ATM, and ATR siRNA, and the expression levels of ATM and ATR were determined using western blot analysis. Control, ATM, and ATR siRNA-transfected HeLa cells were treated with 35 μM MPDB for 15 h. Cell cycle distribution was analyzed by flow cytometry, and the expression levels of protein were determined using western blot analysis. Ratio of relative density was determined by densitometric analysis program (Bio-rad Quantity One® Software) normalized to β-actin. Data are presented as mean ± SD of three independent experiments. $^{***}P < 0.001$ vs. the control group, $^{\#\#}P < 0.01$, $^{\#\#\#}P < 0.001$ vs. the MPDB-treated group.

or not, MRC5 normal human lung fibroblasts and IOSE-80PC immortalized ovarian surface epithelial cells were examined to compare with HeLa cells. Fig. 1A shows that MPDB induced lower cytotoxicity in MRC5 (IC_{50} > 200 μM) and IOSE-80PC (IC_{50} = 147.53 μM) than HeLa (IC_{50} = 38.9 μM), CaSki (IC_{50} = 39.01 μM) and SiHa (IC_{50} = 96.87 μM) cells. In addition, we performed TUNEL assay to further confirm the cell viability of MPDB in HeLa cells. As shown in Fig. 1B, green fluorescent cells indicating apoptotic death were observed and cell viability was significantly decreased by MPDB treatment in HeLa cells. In addition, TUNEL assay revealed that IC_{50} was 37.9 μM indicating a similar value with IC_{50} of MTT assay. These results indicate that MPDB may selectively target cancer cells rather than normal cells, which is crucial for the success of potential cancer preventive agents.

Colony formation is an in vitro cell survival assay that is based on the ability of a single cell to grow into a colony. The assay essentially tests every cell in the population for its ability to undergo “unlimited” division (Franken et al., 2006). Our data revealed that MPDB significantly and concentration-dependently inhibited the colony formation rate (Fig. 1C).

Several studies suggested that resveratrol and its analogs induce cell cycle arrest, leading to cancer cells' death (Kim et al., 2015; Wang et al., 2010; Zielinska-Przyjemska et al., 2017). In previous reports, pterostilbene, a dimethylether analog of resveratrol, was found to possess anti-proliferative effects involving the suppression of G_1 and S phase cell cycle progression (Wang et al., 2010; Zielinska-Przyjemska et al., 2017). To assess whether the anti-proliferative effect of MPDB is caused by perturbation in the cell cycle progression, cell cycle distribution was determined by flow cytometry after staining of the cells with PI. Fig. 1D shows that concomitant with growth inhibitory effects, treatment with 35 μM MPDB for 20 h induced a time-dependent accumulation of cells in G_2/M phase from 28.3 to 67.5%, which was accompanied by a decrease in G_1 phase from 60.1 to 13.5%. However, after 15 h incubation with 35 μM MPDB, the proportion of G_2/M phase was decreased, whereas at 25 h, the sub-G_1 proportion was significantly increased by 36%. These results indicate that treatment with 35 μM MPDB induced G_2/M cell cycle arrest until 15 h, and then followed cell death in HeLa cells.

3.2. MPDB suppressed G_2/M phase-regulatory protein expression in HeLa cells

The Cdc2/cyclinB1 kinase complex, which is considered a main regulator of progression from G_2 to M phase, is regulated by the phosphorylation of specific residues of Cdc2. During the G_2/M transition, Cdc2 is converted into active form by Tyr15 dephosphorylation catalyzed by the Cdc25C tyrosine phosphatase (Senderowicz and Sausville, 2000). In this regard, to gain insights into the molecular mechanism of cell cycle arrest upon treatment with MPDB, levels of G_2/M-regulated proteins were compared by western blot analysis. Treatment of MPDB in HeLa cells resulted in increase of phosphorylations of Cdc2 (Try15) and Cdc25C (Ser216), and protein expression of Wee1 (Fig. 2A). Meanwhile, protein expression levels of CDK2 and Cyclin B1 were not noticeably altered by MPDB treatment in HeLa cells. Treatment of MPDB in HeLa cells induced phosphorylation of Cdc25C (Ser216). Maintaining the Cdc25 phosphatase in a phosphorylated form (Ser216) offers a binding site for 14-3-3 proteins, and results in degradation of Cdc25C protein in the ubiquitin-proteasome system (Levy et al., 2011). Therefore, we investigated the effect of decline in Cdc25C expression by the ubiquitin-proteasome system in MPDB-induced G_2/M cell cycle arrest using a lactacystin, a specific inhibitor of proteasome. The decline in Cdc25C protein levels leading to the phosphorylation of Cdc2 (Tyr15) upon treatment with MPDB was nearly blocked in the presence of lactacystin (Fig. 2B), thus, protecting against MPDB-induced G_2/M arrest (Fig. 2C). These results indicate that the MPDB-induced cell accumulation at G_2/M phase is involved in a proteasome degradation of Cdc25C in HeLa cells.

3.3. MPDB induced phosphorylation of checkpoint kinase and CDKIs in HeLa cells

Chk1 and Chk2 are intermediaries of DNA damage checkpoints, and a major role of these kinases is the triggering cell-cycle arrest to enable DNA repair. Although Chk1 and Chk2 are structurally distinct, they have functionally related kinases that phosphorylate an overlapping pool of cellular substrates (Smith et al., 2010). Because phosphorylation of Cdc25 C at Ser216 is regulated by Chk1 and Chk2, which are intermediaries of DNA damage checkpoints that are activated by the phosphorylation of Ser345 and Thr68, respectively (Bartek and Lukas, 2003), we examined whether MPDB treatment affects the phosphorylation of Chk1 or Chk2 in HeLa cells. After MPDB treatment, phosphorylation levels of Chk1 and Chk2 were increased as early as 5 h, and persisted for the duration of the experiment (Fig. 3A), while levels of Chk1 and Chk2 proteins were not affected by MPDB treatment. In addition, because these two checkpoint kinases act upstream of p53, which lead to the upregulation of CDKIs, such as $p21^{Cip1/Waf1}$ and p27 (Chen and Poon, 2008), we assessed the effect of MPDB on p53, $p21^{Cip1/Waf1}$, and p27 protein levels by western blot analysis. Our data showed a marked and time-dependent increase of p53 phosphorylation at Ser15 and Ser20, and also treatment of MPDB increased the protein expression levels of p53 (Fig. 3B). Moreover, treatment of MPDB resulted in an increase of $p21^{Cip1/Waf1}$ and p27 proteins, compared with control. To verify the role of p53 in G_2/M arrest in MPDB-treated cells, we analyzed cell cycle distribution after knockdown of p53 using siRNA transfection. Fig. 3C shows that the treatment of control siRNA-transfected cells with MPDB resulted in about a 2.5-fold increase in G_2/M phase cells. The MPDB-induced G_2/M arrest was partially but significantly abrogated in p53 siRNA-transfected cells, indicating that p53 is partially involved in MPDB-induced G_2/M arrest.

3.4. MPDB responded to DNA damage involving ATM/ATR activation in HeLa cells

Because phosphorylation of histone H_2AX at Ser139 (γ-H_2AX) is abundant, fast, and correlates well with each double-stranded break, it is the most sensitive marker that can be used to examine the DNA damage produced, and the subsequent repair of the DNA lesion (Sharma et al., 2012). DNA damage activated in response to genotoxic stress in eukaryotic cells is sensed by ATM and ATR, for early signal transmission through the cell cycle checkpoints (Matsuoka et al., 2007). DNA damage activated the two main signaling pathways, which consist of the ATM–Chk2 and ATR–Chk1 protein kinases (Niida and Nakanishi, 2006). When double-strand DNA breaks occur, ATM is activated, which activates Chk2. Western blot analyses revealed that MPDB treatment caused DNA double-strand breaks, as evidenced by identifying phosphorylated histone H_2AX (Ser139) as early as 5 h (http://www.jbc.org/cgi/content/full/279/24/25813 Fig. 4A). In addition, phosphorylation

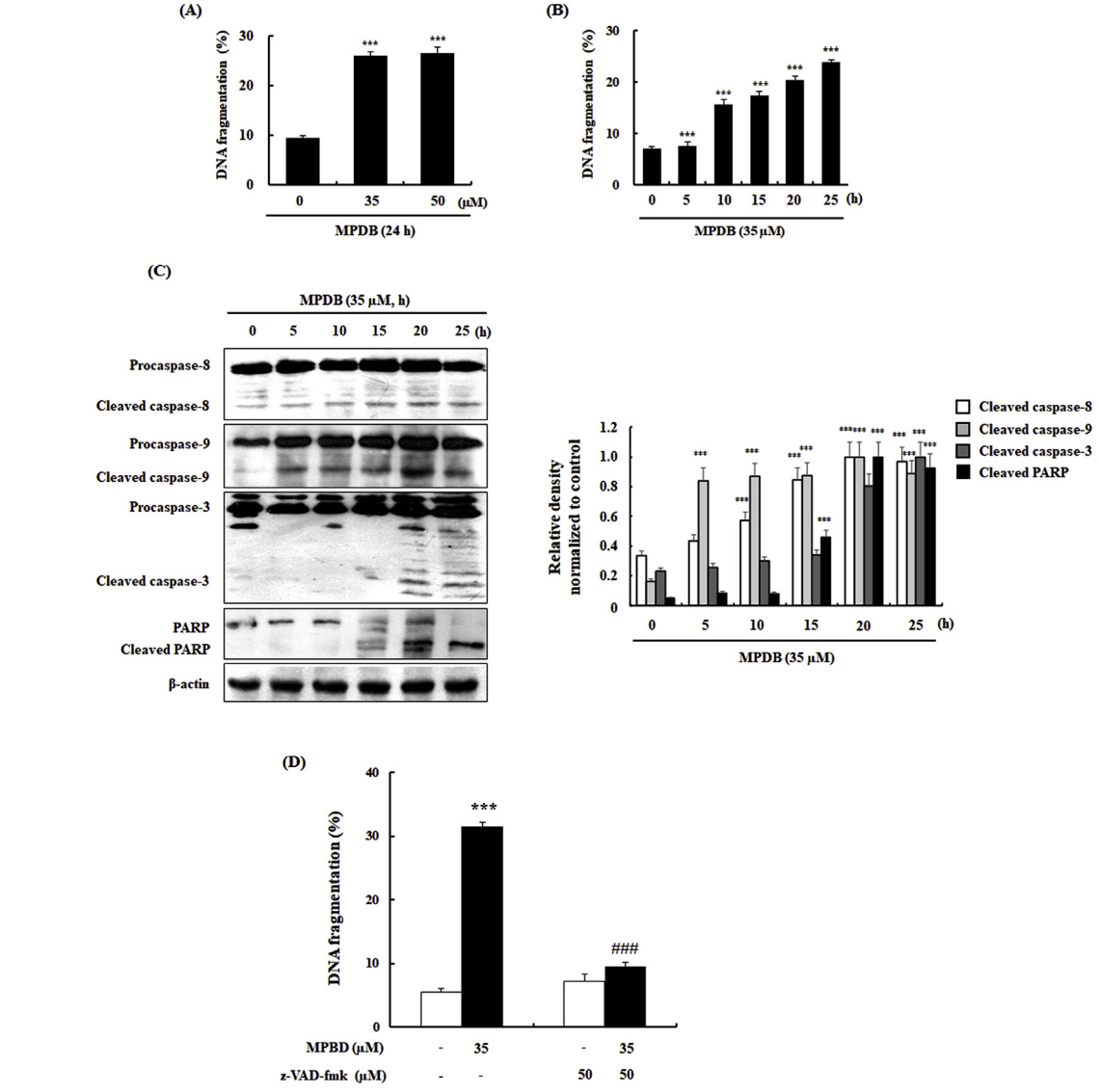

(caption on next page)

Fig. 5. Effect of MPDB on apoptosis induction and apoptosis regulatory protein in HeLa cells. (A and B) HeLa cells were treated with various concentration of MPDB for the indicated time. The extent (%) of DNA fragmentation was determined by fluorometric method using DAPI. (C) The protein expression levels were examined using western blot analysis. β-Actin was used as an internal control. (D) Cells were pretreated for 1 h with or without 50 μM z-VAD-fmk, a broad caspase inhibitor, followed by 35 μM MPDB treatment. After 25 h, the DNA fragmentation was determined by fluorometric method using DAPI. (E and F) The expression levels of representative protein were examined using western blot analysis. Ratio of relative density was determined by densitometric analysis program (Bio-rad Quantity One® Software) normalized to β-actin. Data are presented as mean ± SD of three independent experiments. $^{***}P < 0.001$ vs. the control group, $^{###}P < 0.001$ vs. the MPDB-treated group.

of ATM increased at 5 h, then declined to basal level, whereas in MPDB-treated HeLa cells, phosphorylation of ATR time-dependently increased until 15 h. To identify whether activation of ATM and ATR may play a pivotal role in MPDB-induced G_2/M phase arrest, HeLa cells were transfected with ATM and ATR siRNAs, respectively, followed by examination of the cell cycle distribution and expression levels of G_2/M phase arrest-related protein after MPDB treatment. In the cells transfected with control siRNA, MPDB caused a pronounced G_2/M phase arrest, whereas transfection by ATM or ATR siRNAs attenuated the effect of MPDB- induced G_2/M phase arrest (http://www.jbc.org/cgi/content/full/279/24/25813 Fig. 4B). In addition, down-regulation of ATM and ATR levels prevented MPDB-induced phosphorylation of Cdc2, Cdc25C, Chk1, and Chk2, and expression of CDK inhibitor, $p21^{Cip1/Waf1}$ and p27 in HeLa cells. In line with these observations, Alpna et al. reported that resveratrol upregulated Cdc2 phosphorylation at Try15 via ATM/ATR-Chk1/2-Cdc25C pathway as a central mechanism for DNA damage in ovarian cancer cells (Tyagi et al., 2005). Taken together, these results also suggest that MPDB-induced G_2/M phase arrest, and the activation of Chk1 and Chk2 is dependent on ATM and ATR status, involving DNA damage.

3.5. MPDB-induced apoptosis required the alteration of caspase activities and Bcl-2 protein expression in HeLa cells

Activation of checkpoints in response to DNA damage leads to cell cycle arrest; but in the case of severe damage, apoptotic cell death is followed by cell cycle arrest (Su, 2006). Cell cycle and apoptosis are becoming increasingly appreciated as targets for intervention against cancer. In these regards, resveratrol is a promising agent, as it is capable of eliminating cancer cells by inhibiting cell cycle progression and including apoptosis (Ahmad et al., 2001). Because MPDB treatment with longer incubation times (from 15 to 25 h) significantly increased the Sub-G_1 ratio, we examined whether MPDB induces apoptosis in HeLa cells. Fig. 5A and B shows that MPDB was found to significantly induce DNA fragmentation by DAPI staining in a time-dependent manner.

Execution of apoptosis by various stimuli is initiated by activating either intrinsic or extrinsic pathways, which lead to a series of downstream cascade of events, releasing of various apoptotic mediators from mitochondria, and activation of caspases, important for the cell fate (Ola et al., 2011). In the intrinsic pathway, changes in the induction of Bcl-2 family proteins are closely related to an imbalance in the mitochondrial homeostasis, which leads to apoptosis (Czabotar et al., 2014). In contrast, the extrinsic pathway is triggered by ligand-driven engagement of death receptors leading to the activation of initiator caspase, caspase-8. In this study, treatment with 35 μM MPDB resulted in the proteolytic cleavage of procaspase-3, -8, and -9, indicating caspase activation and cleavage of PARP, a target for caspase-3 during apoptosis (Fig. 5C). The involvement of caspases in MPDB-induced apoptosis was confirmed by using a broad caspase inhibitor, z-VAD-fmk (Fig. 5D). As might have been expected, z-VAD-fmk was able to completely attenuate the MPDB-induced DNA fragmentation, suggesting that MPDB-induced apoptosis is dependent on caspase activation. To further delineate the molecular mechanism of apoptosis by MPDB, we investigated the alteration of intrinsic or extrinsic-related protein expression using western blot analysis. There was no effect on the levels of Bcl-2 expression, whereas the protein levels of Bcl-xl gradually decreased in the MPDB-treated cells (Fig. 5E). Furthermore, we observed cytochrome *c* release into cytosol involving the hyperpolarization of mitochondrial membrane potential. We also detected induction of Fas and Fas-L protein expression in HeLa cells treated MPDB in a time-dependent manner, but the protein levels of FLIP declined (Fig. 5F). Because MPDB resulted in an increase of Fas and Fas-L protein expression and caspase-8 activation, we could suggest that MPDB-induced apoptosis might be provoked by death receptors-mediated caspase-8 activation, leading to cleavage of Bid. Truncated Bid translocates into the mitochondria, causing release of cytochrome *c* and formation of Apaf-1 containing apoptosome. Subsequent caspase-9 activation can then activate effector caspase-3, resulting in apoptosis. Previous report of Lin et al. showed that resveratrol induced apoptosis accompanied by the activation of caspase-3 and -9, and downregulated the expression of the anti-apoptotic proteins Bcl-2 and Bcl-xL in HeLa cells (Li et al., 2018). In line with these reports, resveratrol induced apoptosis via mitochondrial pathway involving caspase activation in various cancer (Kim et al., 2018; Lang et al., 2015; Trincheri et al., 2007). Our data also revealed that MPDB displayed the activation of caspase and decreased Bcl-xL protein expression, indicating mitochondrial apoptotic pathway in HeLa cells. In these regards, we speculated that MPDB, a synthesized analog of resveratrol, is efficient to suppress the proliferation and indicates a similar mitochondrial apoptotic pathway, involving caspase activation in HeLa cells.

4. Conclusions

The current study clearly demonstrates that MPDB has anti-proliferative activity through G_2/M phase arrest by DNA damage being tightly regulated by checkpoint kinases Chk1/Chk2 via ATM/ATR signaling pathway, which in turn triggers apoptosis involving caspase activation and mitochondrial stress in HeLa cells. In conclusion, our findings present MPDB as a potential new chemotherapeutic agent to be considered for further evaluation.

Conflicts of interest

The authors declare no conflict of interests.

Acknowledgements

This research was supported by Basic Science Research Program through the National Research Foundation of Korea funded by the Ministry of Science and ICT (NRF-2017R1A5A2014768) and the Korea Food Research Institute (E0186701).

Transparency document

Transparency document related to this article can be found online at https://doi.org/10.1016/j.fct.2018.11.062.

References

Ahmad, N., Adhami, V.M., Afaq, F., Feyes, D.K., Mukhtar, H., 2001. Resveratrol causes WAF-1/p21-mediated G(1)-phase arrest of cell cycle and induction of apoptosis in human epidermoid carcinoma A431 cells. Clin. Canc. Res. 7, 1466–1473.

Asghar, U., Witkiewicz, A.K., Turner, N.C., Knudsen, E.S., 2015. The history and future of targeting cyclin-dependent kinases in cancer therapy. Nat. Rev. Drug Discov. 14, 130–146.

Azmi, A.S., Bhat, S.H., Hadi, S.M., 2005. Resveratrol-Cu(II) induced DNA breakage in

human peripheral lymphocytes: implications for anticancer properties. FEBS Lett. 579, 3131–3135.
Bartek, J., Lukas, J., 2003. Chk1 and Chk2 kinases in checkpoint control and cancer. Cancer Cell 3, 421–429.
Carter, L.G., D'Orazio, J.A., Pearson, K.J., 2014. Resveratrol and cancer: focus on in vivo evidence. Endocr. Relat. Canc. 21, R209–R225.
Chen, Y., Poon, R.Y., 2008. The multiple checkpoint functions of CHK1 and CHK2 in maintenance of genome stability. Front. Biosci. 13, 5016–5029.
Cho, S.H., Chung, K.S., Choi, J.H., Kim, D.H., Lee, K.T., 2009. Compound K, a metabolite of ginseng saponin, induces apoptosis via caspase-8-dependent pathway in HL-60 human leukemia cells. BMC Canc. 9, 449–461.
Choi, S.Y., Hwang, J.S., Kim, S., Kim, S.Y., 2006. Synthesis, discovery and mechanism of 2,6-dimethoxy-N-(4-methoxyphenyl)benzamide as potent depigmenting agent in the skin. Biochem. Biophys. Res. Commun. 349, 39–49.
Choi, S.Y., Kim, S., Hwang, J.S., Lee, B.G., Kim, H., Kim, S.Y., 2004. Benzylamide derivative compound attenuates the ultraviolet B-induced hyperpigmentation in the brownish Guinea pig skin. Biochem. Pharmacol. 67, 707–715.
Chung, K.S., Choi, J.H., Back, N.I., Choi, M.S., Kang, E.K., Chung, H.G., Jeong, T.S., Lee, K.T., 2010. Eupafolin, a flavonoid isolated from Artemisia princeps, induced apoptosis in human cervical adenocarcinoma HeLa cells. Mol. Nutr. Food Res. 54, 1318–1328.
Czabotar, P.E., Lessene, G., Strasser, A., Adams, J.M., 2014. Control of apoptosis by the BCL-2 protein family: implications for physiology and therapy. Nat. Rev. Mol. Cell Biol. 15, 49–63.
Diaz-Moralli, S., Tarrado-Castellarnau, M., Miranda, A., Cascante, M., 2013. Targeting cell cycle regulation in cancer therapy. Pharmacol. Ther. 138, 255–271.
Estrov, Z., Shishodia, S., Faderl, S., Harris, D., Van, Q., Kantarjian, H.M., Talpaz, M., Aggarwal, B.B., 2003. Resveratrol blocks interleukin-1beta-induced activation of the nuclear transcription factor NF-kappaB, inhibits proliferation, causes S-phase arrest, and induces apoptosis of acute myeloid leukemia cells. Blood 102, 987–995.
Franken, N.A., Rodermond, H.M., Stap, J., Haveman, J., van Bree, C., 2006. Clonogenic assay of cells in vitro. Nat. Protoc. 1, 2315–2319.
Hassan, A.H.E., Choi, E., Yoon, Y.M., Lee, K.W., Yoo, S.Y., Cho, M.C., Yang, J.S., Kim, H.I., Hong, J.Y., Shin, J.S., Chung, K.S., Lee, J.H., Lee, K.T., Lee, Y.S., 2019. Natural products hybrids: 3,5,4'-Trimethoxystilbene-5,6,7-trimethoxyflavone chimeric analogs as potential cytotoxic agents against diverse human cancer cells. Eur. J. Med. Chem. 161, 559–580.
Hydbring, P., Malumbres, M., Sicinski, P., 2016. Non-canonical functions of cell cycle cyclins and cyclin-dependent kinases. Nat. Rev. Mol. Cell Biol. 17, 280–292.
Jang, E., Kim, S.Y., Lee, N.R., Yi, C.M., Hong, D.R., Lee, W.S., Kim, J.H., Lee, K.T., Kim, B.J., Lee, J.H., Inn, K.S., 2017. Evaluation of antitumor activity of Artemisia capillaries extract against hepatocellular carcinoma through the inhibition of IL-6/STAT3 signaling axis. Oncol. Rep. 37, 526–532.
Kim, J.Y., Choi, H.E., Lee, H.H., Shin, J.S., Shin, D.H., Choi, J.H., Lee, Y.S., Lee, K.T., 2015. Resveratrol analogue (E)-8-acetoxy-2-[2-(3,4-diacetoxyphenyl)ethenyl]-quinazoline induces G(2)/M cell cycle arrest through the activation of ATM/ATR in human cervical carcinoma HeLa cells. Oncol. Rep. 33, 2639–2647.
Kim, S.E., Shin, S.H., Lee, J.Y., Kim, C.H., Chung, I.K., Kang, H.M., Park, H.R., Park, B.S., Kim, I.R., 2018. Resveratrol induces mitochondrial apoptosis and inhibits epithelial-mesenchymal transition in oral squamous cell carcinoma cells. Nutr. Canc. 70, 125–135.
Lang, F., Qin, Z., Li, F., Zhang, H., Fang, Z., Hao, E., 2015. Apoptotic cell death induced by resveratrol is partially mediated by the autophagy pathway in human ovarian cancer cells. PLoS One 10, e0129196.
Levy, A., Albiges-Sauvin, L., Massard, C., Soria, J.C., Deutsch, E., 2011. Cell cycle, mitosis and therapeutic applications. Bull. Cancer 98, 1037–1045.
Li, L., Qiu, R.L., Lin, Y., Cai, Y., Bian, Y., Fan, Y., Gao, X.J., 2018. Resveratrol suppresses human cervical carcinoma cell proliferation and elevates apoptosis via the mitochondrial and p53 signaling pathways. Oncol. Lett. 15, 9845–9851.
Matsuoka, S., Ballif, B.A., Smogorzewska, A., McDonald 3rd, E.R., Hurov, K.E., Luo, J., Bakalarski, C.E., Zhao, Z., Solimini, N., Lerenthal, Y., Shiloh, Y., Gygi, S.P., Elledge, S.J., 2007. ATM and ATR substrate analysis reveals extensive protein networks responsive to DNA damage. Science 316, 1160–1166.
Niida, H., Nakanishi, M., 2006. DNA damage checkpoints in mammals. Mutagenesis 21, 3–9.
Ola, M.S., Nawaz, M., Ahsan, H., 2011. Role of Bcl-2 family proteins and caspases in the regulation of apoptosis. Mol. Cell. Biochem. 351, 41–58.
Park, E.Y., Kim, J.I., Leem, D.G., Shin, J.S., Kim, K.T., Choi, S.Y., Lee, M.H., Choi, J.H., Lee, Y.S., Lee, K.T., 2016. Resveratrol analogue (E)-8-acetoxy-2-[2-(3,4-diacetoxyphenyl)ethenyl]-quinazoline induces apoptosis via Fas-mediated pathway in HL-60 human leukemia cells. Oncol. Rep. 36, 3577–3587.
Ramondetta, L., 2013. What is the appropriate approach to treating women with incurable cervical cancer? J. Natl. Compr. Canc. Netw. 11, 348–355.
Rossi, E.L., Khatib, S.A., Doerstling, S.S., Bowers, L.W., Pruski, M., Ford, N.A., Glickman, R.D., Niu, M., Yang, P., Cui, Z., DiGiovanni, J., Hursting, S.D., 2018. Resveratrol inhibits obesity-associated adipose tissue dysfunction and tumor growth in a mouse model of postmenopausal claudin-low breast cancer. Mol. Carcinog. 57, 393–407.
Senderowicz, A.M., Sausville, E.A., 2000. Preclinical and clinical development of cyclin-dependent kinase modulators. J. Natl. Cancer Inst. 92, 376–387.
Sharma, A., Singh, K., Almasan, A., 2012. Histone H2AX phosphorylation: a marker for DNA damage. Methods Mol. Biol. 920, 613–626.
Shukla, Y., Singh, R., 2011. Resveratrol and cellular mechanisms of cancer prevention. Ann. N. Y. Acad. Sci. 1215, 1–8.
Smith, J., Tho, L.M., Xu, N., Gillespie, D.A., 2010. The ATM-Chk2 and ATR-Chk1 pathways in DNA damage signaling and cancer. Adv. Cancer Res. 108, 73–112.
Su, T.T., 2006. Cellular responses to DNA damage: one signal, multiple choices. Annu. Rev. Genet. 40, 187–208.
Torre, L.A., Bray, F., Siegel, R.L., Ferlay, J., Lortet-Tieulent, J., Jemal, A., 2015. Global cancer statistics, 2012. Ca - Cancer J. Clin. 65, 87–108.
Trincheri, N.F., Nicotra, G., Follo, C., Castino, R., Isidoro, C., 2007. Resveratrol induces cell death in colorectal cancer cells by a novel pathway involving lysosomal cathepsin D. Carcinogenesis 28, 922–931.
Tyagi, A., Singh, R.P., Agarwal, C., Siriwardana, S., Sclafani, R.A., Agarwal, R., 2005. Resveratrol causes Cdc2-tyr15 phosphorylation via ATM/ATR-Chk1/2-Cdc25C pathway as a central mechanism for S phase arrest in human ovarian carcinoma Ovcar-3 cells. Carcinogenesis 26, 1978–1987.
Wang, T.T., Schoene, N.W., Kim, Y.S., Mizuno, C.S., Rimando, A.M., 2010. Differential effects of resveratrol and its naturally occurring methylether analogs on cell cycle and apoptosis in human androgen-responsive LNCaP cancer cells. Mol. Nutr. Food Res. 54, 335–344.
Zheng, L.F., Wei, Q.Y., Cai, Y.J., Fang, J.G., Zhou, B., Yang, L., Liu, Z.L., 2006. DNA damage induced by resveratrol and its synthetic analogues in the presence of Cu (II) ions: mechanism and structure-activity relationship. Free Radic. Biol. Med. 41, 1807–1816.
Zielinska-Przyjemska, M., Kaczmarek, M., Krajka-Kuzniak, V., Luczak, M., Baer-Dubowska, W., 2017. The effect of resveratrol, its naturally occurring derivatives and tannic acid on the induction of cell cycle arrest and apopt osis in rat C6 and human T98G glioma cell lines. Toxicol. In Vitro 43, 69–75.